Inelastic processes in K^+-He collisions in energy range 0.7–10 keV

R. A. Lomsadze,[1] M. R. Gochitashvili,[1] R. Ya. Kezerashvili,[2,3] N. O. Mosulishvili,[1] and R. Phaneuf[4]
[1]*Tbilisi State University, Tbilisi, 0128, Republic of Georgia*
[2]*New York City College of Technology, The City University of New York, Brooklyn, New York 11201, USA*
[3]*The Graduate School and University Center, The City University of New York, New York, New York 10016, USA*
[4]*Department of Physics, University of Nevada, Reno, Nevada 89557, USA*
(Received 9 March 2013; published 30 April 2013)

Absolute cross sections for charge exchange, ionization, stripping, and excitation in K^+-He collisions were measured in the ion energy range 0.7–10 keV. The experimental data and the schematic correlation diagrams are used to analyze and determine the mechanisms for these processes. The increase of the excitation probability of inelastic channels with the angle of scattering is revealed. An exceptionally highly excited state of He is observed and a peculiarity for the excitation function of the resonance line is explained. The intensity ratio for the excitation of the K II $\lambda = 60.1$ nm and $\lambda = 61.2$ nm lines is 5:1, which indicates the high probability for excitation of the singlet resonance level $^1P_1$ compared to the triplet level $^3P_1$. The similarity of the population of the $4p$ state of the potassium ion and atom as well as the anomalously small values of the excitation cross sections are explained.

DOI: 10.1103/PhysRevA.87.042710 PACS number(s): 34.80.Dp, 34.50.Fa, 32.80.Zb

I. INTRODUCTION

Ion-atom collisions have been an attractive subject and are of considerable interest in atomic physics due to both their importance in fundamental physics and their application in many fields, such as laboratory and astrophysical plasmas [1], heavy-ion inertial fusion [2], radiation physics, collisional and radioactive processes in Earth's upper atmosphere [3,4], and many other technological areas. In recent decades, ion-atom collisions have been studied in detail experimentally as well as theoretically from low to relativistic collision energies (see, for example, Refs. [1,3,5–7]). There has been an increased need for the evaluation of ion-atom cross sections of different processes for many accelerator applications [8]. For example, a beam interaction with the remaining background gas and gas desorbed from walls limits the intensity of bunches at the RHIC (Relativistic Heavy Ion Collider) [9] and a pressure rise from ion losses at the low-energy antiproton ring brought concerns for the LHC (Large Hadron Collider) [10].

At moderate energies, collisions of closed-shell ions with closed-shell atoms for various inelastic channels such as the ionization, charge exchange, stripping, and excitation are well understood. However, the absolute cross section information of these inelastic processes are of interest, in particular the energy dependence of collisions of K^+ ions with He atoms because the excitation probabilities in these collisions (with some exceptions) are one or two orders of magnitude smaller than in symmetric and quasisymmetric systems [11–14]. Another remarkable feature of inelastic collisions of these closed-shell particles is that the excitation into a doubly excited state occurs with a high probability. Therefore, an accurate determination of the structure of different inelastic cross sections for these collisions is important to understand the mechanisms for inelastic transitions in the outer and, in some cases, inner shells of colliding atomic particles. In order to discuss quantitatively the excitation mechanism one has to evaluate the parameters of existing theories and explore the contributions of separate inelastic channels for the investigated processes by using experimental measurements.

Despite many studies of K^+-He collisions which have been carried out by various methods [11,13–21], available data for the absolute cross sections of the above-mentioned processes are contradictory [11,16,17,20] and, in some cases, unreliable [15].

Charge-exchange cross sections for K^+-Ar, K^+-Kr, K^+-Xe, and K^+-He systems were reported in Ref. [15], using the detection of fast neutral particles within a definite interval of scattering angles. However, as shown in Ref. [22] the restriction on the interval for collision angles in Ref. [15] underestimated the measured charge-exchange cross sections by a factor of ten for the K^+-Ar, Kr, Xe collision pairs over the entire energy range considered. The charge-exchange cross sections reported in Ref. [15] might also have been underestimated for K^+-He collisions. Hence, it was necessary to carry out measurements of the charge-exchange cross sections for K^+-He collisions in a wider and more complete interval of scattering angles using a method that is free of this deficiency.

In Ref. [23], only the absolute value of the cross section for excitation processes, occurring in the case when the mass of the incident ion is less than of target particle (Na^+-Ar) was reported. The results of the measurements of the excitation function in arbitrary units for Na^+-He and K^+-He collision pairs are presented in Refs. [18,19]. The lack of absolute excitation cross sections for the asymmetric K^+-He system motivated the present detailed investigation of the primary mechanisms for this collision process.

In order to make use of the measured cross section for electron production, it is necessary to know absolute ionization cross sections for the target atoms and absolute stripping cross sections for the incident ions. Since there are no previous measurements of the stripping cross section for K^+-He collisions, it is imperative to measure this cross section.

As is known, the basic mechanism responsible for the process of ionization in atomic collisions is a diabatic orbital super promotion into the continuum. Proposed in Ref. [24], this mechanism was further developed in Refs. [25–27].

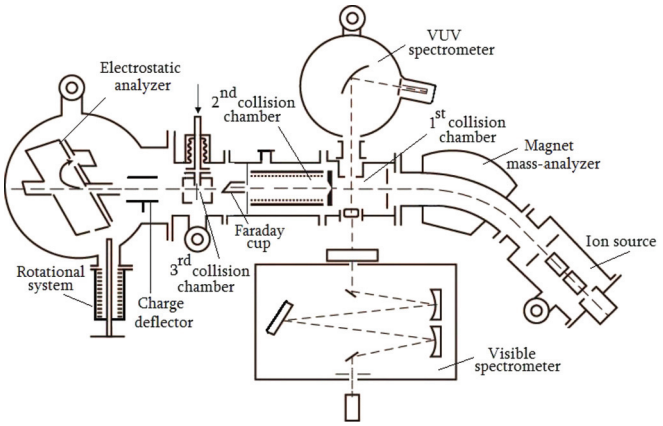

FIG. 1. (Color online) Schematic diagram of the experimental setup.

Advantages and limitations of these studies are assessed for colliding systems with one "active" electron, e.g., H^+-H and He^{2+}-H. It is important to extend the theory to ionization processes in collisions of many-electron atomic systems. Experimental methods [28–30] that are used so far to study this mechanism are based on the measurement of continuous parts of the energy spectra of ejected electrons. More detailed information for the ejected electrons at different impact parameters can be obtained using coincidence techniques.

One of the objectives of this work is to show that in many cases the information extracted from complicated coincidence experiments can also be obtained using a simple method, namely by measuring the energy-loss spectra of incident particles. Such spectra can be measured over a wide range of scattering angles and energy losses, for which the problems of collection of low-energy electrons do not arise. Below, we report absolute total cross sections for charge-exchange processes, ionization, and stripping processes that result in the production of free electrons, as well as the excitation of both the projectile and target particles and energy-loss spectra in collisions of K^+ ions with He atoms.

The remainder of this paper is organized in the following way. In Sec. II we introduce our unique experimental setup, which includes three collision chambers, and present the experimental techniques and procedures used to measure the absolute total cross sections for the excitation, charge-exchange, ionization, and stripping processes. Results of measurements and discussion of mechanisms for different processes occurring in K^+-He collisions are given in Sec. III. Finally, in Sec. IV we summarize our studies and present the conclusions.

II. EXPERIMENTAL TECHNIQUE

A schematic view of the experimental setup is shown in Fig. 1. A beam of K^+ ions from a surface-ionization ion source is accelerated and focused by an ion-optics system, which includes quadruple lenses and collimating slits. After the beam passes through a magnetic mass spectrometer, it enters the first collision chamber containing He gas for measurements of excitation processes in K^+-He collisions. Our setup is designed so that when the beam of K^+ ions passes through the second collision chamber measurements of the charge-exchange, ionization, and stripping processes occur. The energy-loss spectrum is obtained by a collision spectroscopy method when K^+ ions collide with target He atoms in the third collision chamber. The pressure in each collision chamber when there is no He target gas is kept below 10^{-6} Torr and the typical pressure under operation is 10^{-4} Torr. The measurements are performed under a single-collision conditions. The current of primary ions in the collision chamber is $I = 0.01$–0.1 μA. The uniqueness of our experimental approach is that the quality of the beam as well as the experimental conditions for all processes under investigation always remain identical. Moreover, the experimental techniques include a condenser-plate method, angle- and energy-dependent collection of product ions, energy loss, and optical spectroscopy under the same "umbrella." The measurement procedures have been discussed in some detail previously [23,31–33]; therefore, the description of the present measurements can be kept comparatively short.

A. The first collision chamber

The measurements of the excitation processes in K^+-He collision were performed when the beam of K^+ ions passed through the first collision chamber. Cross sections for the excitation processes were measured by the optical spectroscopy method [33]. The radiation emitted in the first collision chamber was observed at an angle of 90° with respect to the direction of the primary ion beam. The spectral analysis of this radiation was performed in the vacuum ultraviolet (VUV) as well as visible spectral regions. An electron multiplier was used to detect the intensity of the radiation. Particular attention was devoted to the reliable determination and control of the relative and absolute spectral sensitivity of the light-recording system. This was done by measuring the signal due to the emission of molecular bands and atomic lines excited by electrons in collisions with H_2, N_2, O_2, and Ar. For this, an electron gun was placed directly in front of the entrance slit of the collision chamber. The relative spectral sensitivity, and the values of the absolute cross sections, were obtained by comparing the cross sections for the same lines and molecular bands reported in the literature [34–38]. The uncertainties in the excitation cross sections for the K^+-He system are estimated to be 20% and the uncertainty of the relative measurements does not exceed 5%.

B. The second collision chamber

When the K^+ beam enters the second collision chamber filled with the target gas, the measurements for the charge-exchange and ionization processes occur. The charge-exchange and ionization cross sections were measured by a refined version of the capacitor method [31]. In an earlier paper [15] the measurements were performed by the standard transfer electric field method. The customary procedure is to use one of the central electrodes as the measurement electrode. We consider that such an approach is the reason for significant errors in measurements [15] because scattered K^+ ions may strike the electrodes used for measurements. This effect becomes more evident especially for low-energy collisions.

To avoid this deficiency we accordingly used a refined version of the transfer electric field method in which the effect of scattering on the measured results is substantially reduced by shifting from the central electrode (standard method) to the first electrode (towards beam entrance side). Due to fringing effects at the edges of this electrode a system of auxiliary electrodes between the first electrode and the entrance slit was installed. These auxiliary electrodes create a uniform potential near the first electrode. The first electrode, the auxiliary electrodes, and the entrance slit are all positioned as close together as possible. This close arrangement limits the scattering region on the beam to the entrance side. Thus, according to our estimation, taking into account the geometry of our facilities, only those ions which are scattered through angles greater than 70° can reach the electrodes.

The primary ions are detected by the Faraday cup. Collision particles (secondary positive ions and free electrons) are detected by a collector. The collector consists of two rows of plate electrodes that run parallel to the primary ion beam. A uniform transverse electric field, responsible for the extraction and collection of collision particles, is created by the potentials applied to the grids. This method yields direct measurements of the cross sections σ^+ for the production of singly positively charged ions and σ^- for electrons as the primary beam passes through the gas under study. These measured quantities are related in an obvious way to the capture cross section σ_c and the apparent ionization cross section σ_i and are determined as

$$\sigma^+ = \sigma_c + \sigma_i, \qquad \sigma^- = \sigma_s + \sigma_i. \tag{1}$$

In (1) σ_s is the cross-section stripping of the incident ion. The cross section σ_i is always larger than the cross section for stripping σ_s.

The uncertainty in the measurements of the absolute values of the cross sections σ^+ and σ^- is estimated to be 15% over the entire energy interval studied. This is determined primarily by the uncertainty in the measurement of target gas pressure in the collision chamber. The uncertainty in the measurement of the ionization cross section σ_i is estimated to be ∼20% over the entire energy range. The larger value in comparison with that for the measurement of the cross section σ^- is a consequence of the presence of an additional error in the measurements of σ_i due to stripping of K^+ ions. At K^+ energies less than 2.0 keV the cross section σ^+ is significantly larger than σ^-. Accordingly, the error in the determination of the capture cross section σ_c in this energy region is determined primarily by the error in the measurement of σ^+. With increasing K^+ energy the cross sections σ^+ and σ^- become more nearly equal. As a result the error in the determination of σ_c increases. At a K^+ energy of 5 keV it is estimated to be 25%.

The stripping cross sections were measured in an independent experiment. A beam of K^+ ions from a surface-ionization ion source after acceleration and focusing passes through the second collision chamber. It is then analyzed for the charge composition by an additional 90° magnetic mass spectrometer (not shown in Fig. 1). A set of slits that was located in front of the detector enables the profile of the projectile beam to be scanned in detail. The ratio of the number of doubly charged ions, produced as a result of stripping, to the incident ion beam, K^{2+}/K^+, is determined from the areas under the corresponding lines in the mass spectrum. Since inelastic processes, apparently including stripping, may be accompanied by the scattering of particles through comparatively large angles in collisions between alkali-metal ions and inert gas atoms [12,13,22], special measures were taken to arrange complete collection of K^{2+} ions.

C. The third collision chamber

The energy-loss spectrum was obtained by the collision spectroscopy method [32]. The primary beam extracted from the ion source was accelerated to the desired energy before being analyzed according to q/m (q and m are the ion's charge and mass, respectively). The analyzed ion beam was then allowed to pass through the third collision chamber by appropriately adjusting the slits prior to entering into a "box" type electrostatic analyzer. The energy resolution of this analyzer is $\Delta E/E = 1/500$. Automatic adjustments of analyzer potentials gave the possibility for investigation of energy-loss spectra in the energy range of 0–100 eV. The differential cross section is measured by rotating the analyzer around the center of collisions over an angular range between 0° and 25°. The laboratory angle is determined with respect to the primary ion beam axis with an accuracy of 0.2°.

For the measurements of the charge-exchange differential cross section the charge component of scattered primary particles realized in the third collision chamber is separated by the electric field (see ion charge deflector in Fig. 1) and neutral particles formed by electron-capture collisions are registered by the secondary electron multiplier. Such a tool gives us the possibility to determine total cross sections and compare them with the results obtained in the second collision chamber. In addition, the measured energy-loss spectrum gives detailed information related to the intensity of inelastic processes realized in the first collision chamber (excitation) and in the second collision chamber (charge exchange, ionization, and stripping).

III. RESULTS OF MEASUREMENTS AND DISCUSSION

The collision of a K^+ ion beam with He gas leads mainly to the following processes: charge-exchange reaction,

$$K^+ + He \rightarrow K + He^+, \tag{2}$$

when the K atom and He^+ ion can be in the ground state or in different excited states; different excitation processes,

$$K^+ + He \rightarrow K^{+*} + He^*, \tag{3}$$

which include different channels for excitation of the K^+ ion or/and He atom; stripping of K^+,

$$K^+ + He \rightarrow K^{2+} + He + e, \tag{4}$$

and ionization of He

$$K^+ + He \rightarrow K^+ + He^+ + e, \tag{5}$$

that include different channels for excitation of the K^+ ion or/and He^+ ion, as well as excitation of autoionization states

$$K^+ + He \rightarrow K^+ + He^{**} \rightarrow K^+ + He^+ + e, \tag{6}$$

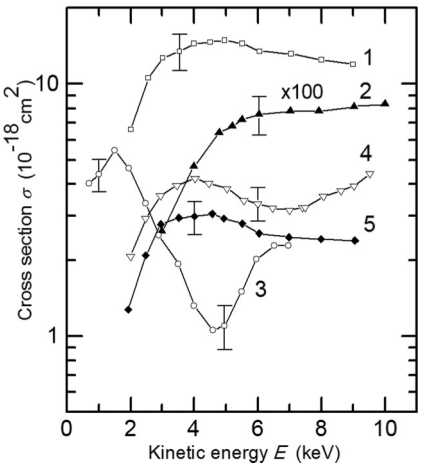

FIG. 2. Dependencies of excitation cross sections and total charge-exchange cross sections on energy of the K^+ ion in K^+-He collisions. Curves: (1) K II ($\lambda = 60.1$ nm) for process (3); (2) K I ($\lambda = 766.5$ nm) for process (2); (3) charge-exchange process when K is in the ground state in process (2); (4) He I ($\lambda = 58.4$ nm) for process (3); (5) K II ($\lambda = 61.2$ nm) for process (3).

when He^{**} is formed in different autoionization states such as doubly excited states ($2s^2$), ($2p^2$), and ($2s2p$) and then decays by emitting an electron.

In Figs. 2–4 the measured energy dependencies of absolute total cross sections are presented for charge exchange into the ground and excited states of K^+, the ionization, stripping, and excitation function of potassium atom, ion, and target helium atom in K^+-He collisions. Figures 5(b)–5(d) represent a typical example of the energy-loss spectrum for K^+-He systems. For comparison, in Fig. 5(a) is given the energy-loss spectrum for K^+-Ar collisions. We have also measured the energies of the electrons emitted in the collisions. It was found that the energy of most liberated electrons is below 10–15 eV.

As seen from Figs. 2 and 3, a distinctive feature of most of these inelastic processes is the small magnitude of the

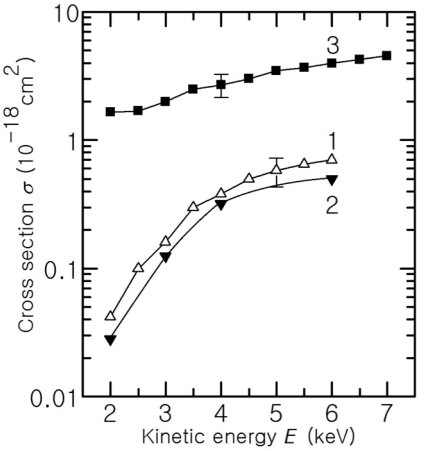

FIG. 3. The absolute cross section for $K^+ +$ He collisions. The formation of K^{2+} product ions is shown by curve 1. Results of calculations of the production of K^{2+} in $K^+ +$ He collisions from Ref. [25] are indicated by curve 2. Curve 3 indicates the free electron production in $K^+ +$ He collisions.

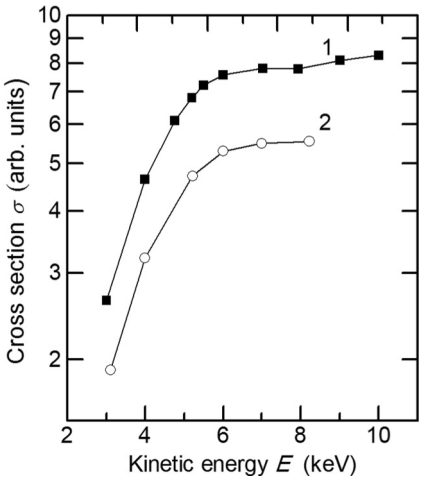

FIG. 4. The excitation functions for the potassium atom K and ion K^+ in K^+-He collisions. (1) KI, $\lambda = 766.5$ nm; (2) KII, $\lambda = 389.8$ nm.

cross section. The excitation functions of the K II lines at $\lambda = 60.1$ nm and $\lambda = 61.2$ nm are similar (curves 1 and 5 in Fig. 2). The curves did not differ in shape and curve 1 could be obtained from curve 5 by multiplying the ordinate of the last one by a factor of ~5. Another feature that is prominent in the ionization, charge-exchange, and excitation cross sections is the difference in the energy dependencies. While the ionization cross section (Fig. 3) and excitation function of the K^+ ion (Fig. 2, curve 5) and K atom (Fig. 2 curve 2) are small at low energies and increase monotonically with energy up to 5 keV, the total charge-exchange cross section has a complex energy dependence and generally decreases with the collision energy up to 5 keV and then increases (Fig. 2, curve 3). Structural features are also observed in the resonance line for the helium atom (Fig. 2, curve 4).

Distinct features are observed in the energy-loss spectra shown in Figs. 5. In the case for which colliding particles have nearly equal masses [K^+-Ar, Fig. 5(a)] the main inelastic process is realized effectively in the 10- to 35-eV energy-loss interval, while for asymmetric colliding pairs [K^+-He, Fig. 5(d)] these energy losses are extended up to 60 eV.

The data obtained in this study can be used to draw certain conclusions about the possible reasons for these features in the cross sections and mechanisms for the corresponding processes. To explain these mechanisms we use a schematic correlation diagram of the adiabatic quasimolecular terms for the system of colliding particles. The diagram was constructed based on Barat-Lichten rules [39] and is presented in Fig. 6.

A. Excitation functions

These results motivate us to explore the excitation functions for collisions of K^+ ions with helium atoms. The radiation generated in these collisions is shown in Fig. 2 and it includes one resonance line of the K atom at $\lambda = 766.5$ nm (curve 2) corresponding to the channel $K^+(3p^6) + He(1s^2) \rightarrow K(4s) + He^+(1s)$ of process (2), two resonance lines of the K^+ ion at $\lambda = 60.1$ nm (curve 1) and $\lambda = 61.2$ nm (curve 5) for process (3), and one resonance line of the He atom at

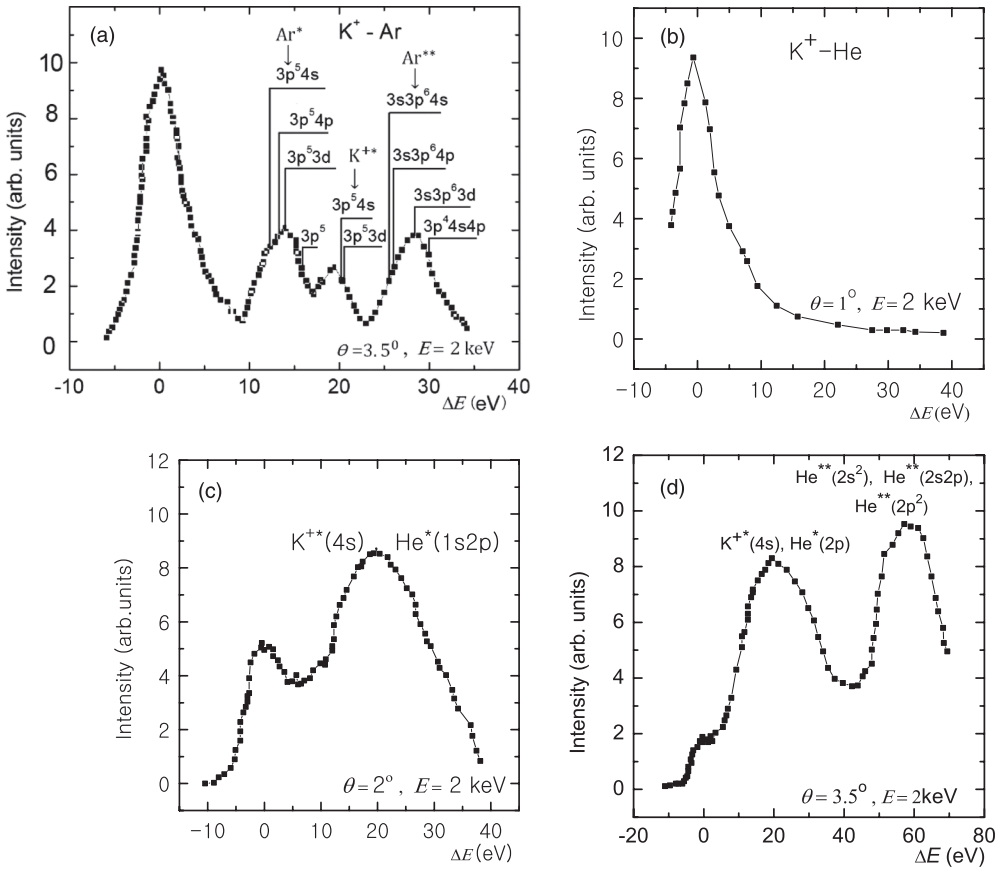

FIG. 5. Energy-loss spectra. (a) The energy-loss spectrum for K^+-Ar collision. (b)–(d) Energy-loss spectra for K^+-He collisions at different scattering angles.

$\lambda = 58.4$ nm (curve 4) corresponding to different channels of process (3).

The K II $\lambda = 60.1$ nm line representing a transition from the $^1P_1(3s^2 3p^5[^2P_{1/2}]^0 4s')$ level to the ground state $^1S_0(3s^2 3p^6)$ is much stronger than the $\lambda = 61.2$ nm line, corresponding to transitions from the state $^3P_1(3s^2 3p^5[^2P_{3/2}]^0 4s)$ to the ground state. The intensity ratio of the K II $\lambda = 60.1$ nm and $\lambda = 61.2$ nm lines shown in Fig. 2 is 5:1, indicating that the probability of excitation of the singlet resonance level $^1P_1$ is greater than that of the triplet level $^3P_1$, due to spin conservation.

Curve 4 in Fig. 2 for the excitation function of the $He(1s2p)$ resonance line for the channel $K^+(3p^6) + He(1s^2) \rightarrow K^+(4p) + He(1s2p)$ has unusual energy dependence. This results from the overlapping of different excitation channels in different energy ranges. Particularly, the analysis of the correlation diagram in Fig. 6 leads to the conclusion that at relatively small energies the excitation of $He(1s2p)$ originate due to the exchange interaction through the intermediate state corresponding to the channel $K^+(3p^6) + He(1s^2) \rightarrow K(4s) + He^+(1s)$, while at large energies the excitation of $He(1s2p)$ may occur due to the Σ-Π transition between terms which correspond to the $K^+(3p^6) + He(1s^2) \rightarrow K^+(4s') + He(1s^2)$ and $K^+(3p^6) + He(1s^2) \rightarrow K^+(3p^6) + He(1s2p)$ channels.

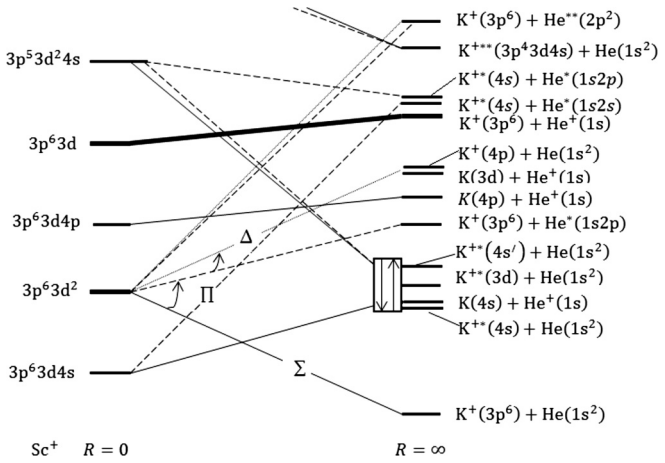

FIG. 6. Schematic correlation diagram.

B. The charge-exchange reaction

In determining the processes responsible for charge exchange in K^+-He collisions, we compare the total charge-exchange cross sections presented in Fig. 2 by curve 3 with those corresponding to the decay of resonant levels of the potassium atom presented by curve 2. Taking into account the selection rules and the ratio of oscillator strengths for the transitions, we show that the decay of any of the excitation levels of the potassium atom culminates in about half the cases with a transition of the atom to a resonant state, which then

decays. According to our data, the decay cross section of the resonant levels of the potassium atom in K^+-He collisions increases with incident ion energy, reaching about 2×10^{-20} cm^2 at an ion energy of 3 keV and 7×10^{-20} cm^2 at 5–7 keV. At low collision energies these cross sections are less than 1%, and at high collision energies they are ~5% of the total charge-exchange cross sections. It follows that in these collisions the cross section for the capture of an electron to an excited state of atom through the channels $K^+(3p^6) + He(1s^2) \rightarrow K(4p) + He^+(1s)$ or $K^+(3p^6) + He(1s^2) \rightarrow K(3d) + He^+(1s)$ is less than 10% of the total charge-exchange cross section. In other words, the charge-exchange process results primarily from capture of an electron to the ground state of the K atom. The target ions are produced in these processes primarily in the ground state. Processes involving capture accompanied by excitation of the resultant target ion He^+ make a small contribution into the charge-exchange cross section, apparently because the energy defect of these processes is of the same order of magnitude as the collision energy (the total kinetic energy of the particles in the c.m. system) [40]. The energy defect of these processes is ~61 eV, while the collision energy at an ion energy of 700 eV is only 65 eV in the c.m. system. We thus can conclude that the charge-exchange reaction (2) is governed primarily by the capture of an electron in the ground state of the potassium atom, accompanied by the formation of a helium ion also in the ground state: $K^+(3p^6) + He(1s^2) \rightarrow K(4s) + He^+(1s)$. This process can occur, as can be seen from the diagram in Fig. 6, as a result of the direct pseudocrossing of the term corresponding to the state $K(4s) + He^+(1s)$ with the ground state of the system. Since the $K(4s) + He^+(1s)$ state has only Σ symmetry, it follows that Σ-Σ transitions play a dominant role in the charge-exchange processes.

Since the mass of projectile K^+ is much larger than that of the He target, a significant decrease in the velocity of the relative motion of the particles when traversing the pseudocrossing region occurs at significantly large initial ion energies (of the order of 1 keV), unlike for systems with comparable masses. In this situation, the only particles which can approach each other to a distance at which the terms undergo a pseudocrossing are those for which the impact parameters are much smaller than this distance. The small value of the charge-exchange cross section in K^+-He collisions compared to those for collisions of certain other pairs of particles, e.g., K^+-Ar, K^+-Kr, K^+-Xe, at ion energies 0.7–10.0 keV, can be attributed precisely to this effect [31]. For these pairs of particles, the mass of the incident particle is less than or roughly equal to the mass of the target particle. Therefore, there is no significant decrease in the relative velocity compared to the initial velocity of the ion. Correspondingly, there is no significant decrease in the impact parameters at which the pseudocrossing regions are reached.

In the two-channel approximation, the charge-exchange cross section should increase with increasing of ion energy, approaching the maximum value $\sigma_{max} \sim 0.5\pi R_0^2$, where R_0 is the position of the pseudocrossing region [1]. Using a limiting value of 65 eV as the interaction energy of the particles in the pseudocrossing region, and the potential curve for the ground state of K^+-He system from Ref. [41], we find $R_0 \approx 0.7$ Å and correspondingly, $\sigma_{max} \approx 0.7 \times 10^{-16}$ cm^2. It can be seen from Fig. 2 (curve 3) that the cross section actually increases (up to $\sigma = 5.5 \times 10^{-18}$ cm^2) with increasing of the ion energy only up to 1.5 keV. As the energy further increases, the cross section decreases, and it increases again only at energies greater than 5 keV. This behavior of the cross section indicates that at the ion energy of 1.5 keV the charge-exchange mechanism is not correlated exclusively with the interaction of the entrance and exit channels, since the interference of these channels with other channels becomes important. In particular, the decrease of the cross section at ion energies 1.5–5.0 keV can be related to the interference of the exit channel with the channel asymptotically dissociating into to the state $K^+(3p^5 4s') + He(1s^2)$, as follows from Fig. 6. An interaction of these channels is confirmed by the agreement of the position of the minimum in the energy dependence of the charge-exchange cross section with the position of the maximum in the energy dependence of the cross section for the decay of the resonant level of the ion $K^+(3p^5 4s')$, shown in Fig. 2. The position of the maximum value of the cross section 1.5×10^{-17} cm^2 (see Fig. 2, curve 1) corresponds roughly to that of the dip in the charge-exchange cross section.

C. The ionization process

It follows from the results of present measurements of emitted electrons in K^+-He collisions and, in part, from the data obtained in Ref. [42], where the electron spectrum was measured over the interval 5–24 eV, that the liberation of slow electrons (with energies less than 10–15 eV) is a characteristic of ionization (5) in K^+-He collisions. In order to determine the channel and mechanism of ionization, we estimate the contribution of several inelastic processes that result in emission of slow electrons. The contribution of the direct ionization $K^+(3p^6) + He(1s^2) \rightarrow K^+(3p^6) + He^+(1s) + e$, that in the quasimolecular model is linked to the transition of the adiabatic term into the continuum, is estimated following Ref. [25]. The expression given in Ref. [25] is written in terms of the principal quantum number for a hydrogenlike atom. Therefore, we modify it slightly for the estimation of the cross section for the emission of electrons from multielectron atoms. Then the final expression can be written as

$$\sigma = 2\pi v k \frac{|R_{nl}|^2}{E_{nl}} \mathrm{Im}R_{nl} \exp(-2E_{nl}\mathrm{Im}R_{nl}/v), \qquad (7)$$

where v is the relative velocity of the particles in the nonadiabatic region, k is the number of electrons within the united atom in the state with quantum numbers (n,l), E_{nl} is the binding energy of an electron in the nonadiabatic region, and $\mathrm{Im}R_{nl}$ and $\mathrm{Re}R_{nl}$ are the coordinates where the potential surfaces cross in the complex plane. They are

$$\mathrm{Im}R_{nl} = \frac{\sqrt{2l(l+1)}}{Z_{\mathrm{eff}}}, \quad \mathrm{Re}R_{nl} = \frac{l(l+1)}{Z_{\mathrm{eff}}} \quad (m = 0), \qquad (8)$$

where Z_{eff} is the effective charge of the nucleus of the united atom. The last formula was derived by the same approach as the expression (26) in Ref. [25], except that the population of the initial orbital is taken into account, and the binding energy is introduced as a parameter.

Analysis of the correlations of the molecular orbital in the $(KHe)^+$ system shows that in the united atom limit, the 1*s*

electrons of the He atom become $3d$ electrons of the Sc^+ ion. Since this result is of importance for evaluating the contribution of the direct ionization, we note that it agrees with both the Barat-Lichten correlation rules [39] and the Eichler-Wille rules [43]. Consequently, the value $l = 2$ was chosen for the evaluation of the cross section. The binding energy E_{nl} of the electrons in the nonadiabatic region was chosen to be equal to that of the $3d$ electrons of the Sc^+ ion. The effective charge Z_{eff} was determined by the interpolation of the data of Ref. [44]. For the $3d$ electrons of the Sc^+ ion, the value $Z_{\text{eff}} = 5.5$ was found. Estimates of the cross section for the direct ionization with these parameters show that at an ion energy of 2.5 keV the contribution of the direct ionization to the total ionization cross section is less than 0.1%, while at 6.5 keV it is less than 5.5%; i.e., this contribution is insignificant over the entire energy range studied.

The double ionization of the He atom and capture accompanied by ionization of the He atom evidently make a small contribution to the ionization cross section. There are two reasons for this: the large energy defect for these processes, 79 and 74.6 eV, respectively, and the absence of pseudocrossings of the corresponding quasimolecular terms with the ground-state term, as follows from the diagram in Fig. 6.

As follows from the electron spectrum in Ref. [42], the resultant intensity of the discrete lines associated with capture to the autoionization states of the K atom and ultimately corresponding to the ionization of the He atom is several times lower than that of the lines of the K^+ ion corresponding to stripping processes. Since the stripping cross section is less than 10% of that for ionization (see Fig. 3) we find that the capture to autoionization states of K atoms also plays no important role in the ionization. Consequently, by systematically evaluating the contributions of various inelastic processes to the ionization of the target atoms in K^+-He collisions, we find that the ionization may be caused primarily by the decay of quasimolecular autoionization states. These could be expected to be states with two excited electrons [see the energy-loss spectrum in Figs. 5(c) and 5(d)], since such states undergo quasimolecular decay with a high probability, liberating mainly slow electrons with a continuous energy distribution [30]. Both of these circumstances agree with the conclusions which follow from an analysis of the correlation diagram of the system, and they add a few refinements to the ionization mechanism.

It can be seen from the diagram that the ground state of the system goes over in the limit of the united atom into the $3p^6 3d^2$ ($^1D_2$) singlet state of the Sc^+ ion. Below this state, the Sc^+ ion has only three triplet states (not shown in the diagram) and one singlet state (with the configuration $3p^6 3d 4s$) [45]. Only the term, asymptotically dissociating into $K(3p^6 4s) + He^+$, with the appropriate $^1\Sigma$ symmetry, crosses the ground state. Note that electron transitions occur primarily between terms of the same multiplicity. We find that the autoionization results from the filling of primarily terms of $^1\Pi$ and $^1\Delta$ symmetry. These terms correlate in the limit of separated atoms to the states: $K^{+*}(4s) - He^*(1s2s)$, $K^{+*}(4s) - He^*(1s2p)$, $K^{+**}(3p^4 3d 4s) - He(1s^2)$, and $K^+(3p^6) - He^{**}(2p^2)$ (Fig. 6). All of these terms, as expected, correspond to two-electron excitations of the system. Since the ground-state term has the symmetry $^1\Sigma$, the terms are populated as a result of Σ-Π and Σ-Π-Δ transitions, associated with the rotation of the internuclear axis along the different nuclear trajectories.

D. The stripping process

According to our estimates, the governing mechanism for the stripping process (4) is the transition of adiabatic term into the continuum. The stripping cross section determined by this mechanism was calculated using Eqs. (7) and (8). As it follows from the diagram in Fig. 6 the $3p$ electrons of the K^+ ion are correlated with the $3p$ electrons of the Sc^+ ion. Consequently, in evaluating the cross section we selected $l = 1$, while we took Z_{eff} to be the same as for the $3d$ electrons of an Sc^+ ion in evaluating the ionization cross section. The stripping cross section calculated with these parameters is consistent over the entire energy region (Fig. 3, curve 1) with the experimental cross section (Fig. 3, curve 2) to within less than 25%. Although this agreement is fortuitous to some extent, it does support the conclusion that this is the governing mechanism for the stripping: $K^+(3p^6) + He(1s^2) \rightarrow K^{2+}(3p^5) + He(1s^2) + e$.

E. The excitation function of K atom and K^+ ion

As shown in Fig. 4, the excitation functions of the K atom and K^+ ion for $4p$ lines are similar, apparently indicating a common mechanism of population. For the interpretation of this result it is expedient to use the correlation diagram of molecular states of the $(KHe)^+$ system from Fig. 6. We emphasize that the term corresponding to the $K(3d)$ state is responsible for both the population of the potassium atom and the ion into the $4p$ state. The terms corresponding to the excitation of $K(4p)$ as well as $K^+(4p)$ do not have immediate crossing points with the entrance term $K^+(3p^6) - He(1s^2)$. However, both of these terms may be populated from that corresponding to $K(3d)$ excitation states by means of a double rotational transition Σ-Π-Δ between the entrance term and that corresponding to the $K(3d) - He^+(1s)$ state. The excitation state of the term corresponding to $K(4p)$ may be populated from the term corresponding to the $K(3d)$, via the cascade transition, from level $3d$ to $4p$. As for the population of the term $K^+(4p)$, because the term $K^+(4p) - He(1s^2)$ and $K(3d) - He^+(1s)$ at large internuclear distance are energetically closed (the energy defect is 0.4 eV), the exchange interaction between these states may cause a population of the term corresponding to $K^+(4p)$, and hence the identical energy dependencies of the cross sections. The probability of population of the $K(3d)$ level of the potassium atom itself is very small, due to the small probability of the Σ-Π-Δ transition (see Fig. 6). Perhaps this is the reason for the anomalous small excitation cross section of the potassium atom in the $K(4p)$ state and for the $K^+(4p)$ state. This can be seen from Fig. 2, curve 2, and Fig. 4, curves 1 and 2, respectively.

F. The energy-loss spectrum

Another conclusion that can be drawn from Fig. 5 is that the energy-loss spectra for both K^+-Ar and K^+-He collisions have a discrete character. The energy-loss spectrum for K^+-Ar in Fig. 5(a) is presented for comparison and is chosen for

the fixed energy ($E = 2$ keV) and scattering angle ($\theta = 3.5^\circ$) at which the inelastic channels are most populated. The first peak of this spectrum corresponds to the elastic scattering of K^+ ions, while the second one corresponds to the single electron excitation of the Argon atom to $(4s)$, $(4p)$, and $(3d)$ states with energy losses of $11.6 < \Delta E < 14$ eV. The third one corresponds to the excitation of K^+ ions into the $(4s)$ and $(3d)$ states with energy losses $16 < \Delta E < 22$ eV, and the fourth one corresponds to the single and double autoionization states of Ar with energy losses $25 < \Delta E < 32$ eV.

The energy-loss spectrum for K^+-He colliding pairs is given at $E = 2$ keV and for the various scattering angles of K^+ ions: $\theta = 1^\circ$, Fig. 5(b); $\theta = 2^\circ$, Fig. 5(c); $\theta = 3.5^\circ$, Fig. 5(d), respectively. This allows us to observe the dynamics of inelastic channels. Let us analyze the energy-loss spectrum for the K^+-He pair at the ion energy of $E = 2$ keV and $\theta = 3.5^\circ$ scattering angle shown in Fig. 5(d). The first maximum at zero energy loss is attributed to the elastic scattering of K^+ ions. The second maximum at $\Delta E = 20$–21 eV is ascribed to the excitation of the potassium ion into the $(4s')$ states and to the direct excitation of the helium atom into $(2p)$ state. With low probability of excitation ionization and stripping, with energy losses $\Delta E = 24.6$ eV and $\Delta E = 31$ eV, respectively, are favored. Rather higher excitation probabilities are observed at the energy loss $58 < \Delta E < 60$ eV and they are ascribed to the two electron excitation of the helium atom into $(2s^2)$ and $(2p^2)$ states [46,47].

The remarkable feature of the spectrum from Figs. 5(b)–5(d) is the rapid decrease of the elastic channel intensity with scattering angle. This fact indicates the increasing importance of inelastic channels. In spite of the fact that the energy-loss spectrum has been measured up to 60 eV, a significant elastic peak was observed only at 1° scattering angle. With the increase of scattering angle from 1° to 3.5°, the excitation of the inelastic channel (one- and two-electron excitation of helium atom and excitation of potassium ion) becomes predominant. We have also observed these specific features of the energy-loss spectrum for other energies of the incident ions. This allows us to conclude that for K^+-He collisions in this energy range, the main inelastic channel is the excitation of the K^+ ion into the $(4s')$ state. This result was also confirmed from our excitation function given in Fig. 2, curve 1. Indeed, as seen from this figure, the intensities of excited $K^+(4s')$ lines are more than one order higher than for the rest of the inelastic channels considered here.

IV. CONCLUSION

Using refined experimental methods that include a condenser plate method, angle- and energy-dependent collection of product ions, energy loss, and optical spectroscopy under the same umbrella and a well-checked calibration procedure of the light recording system, we have measured the absolute values of the charge-exchange, ionization, stripping, and excitation cross sections. The correlation diagram of the $(KHe)^+$ system has been employed to discuss the mechanisms for these processes in the K^+ ion energy range 0.7–10 keV.

Charge exchange in K^+-He collisions mostly occur through the channel $K^+(3p^6) + He(1s^2) \rightarrow K(4s) + He^+(1s)$ resulting from the capture of the electron to the ground state of the atom in regions of pseudocrossings of the potential curves of $^1\Sigma$ symmetry.

The primary ionization mechanism in K^+-He collisions is the filling, as a result of Σ-Π and Σ-Π-Δ transitions, of quasimolecular autoionization terms and their decay in the region of the transition into the continuum (in the stage in which a quasimolecule exists).

Stripping in K^+-He collisions occurs via a mechanism involving a transition of adiabatic term into the continuum in the region of a nonadiabatic interaction of molecular orbitals with orbital angular moments which are identical in the limit of the united atom.

A common mechanism of the populations, as well as the small values of excitation cross sections for the potassium ion and atom into $4p$ states are explained. The usage of the collision spectroscopy method has permitted us to observe exceptionally highly excited states of helium atom in the energy-loss spectrum.

ACKNOWLEDGMENTS

The authors are grateful to Professor A. Müller for valuable and stimulating discussions. This work was supported by the Georgian National Science Foundation (Reference No. FR/219/6-195/12) under Grant No. 31/29.

[1] E. E. Nikitin and S. Ya. Umanskii, *Theory of Slow Atomic Collisions* (Springer, Berlin-Heidelberg, 1984).
[2] B. G. Logan *et al.*, Nucl. Instrum. Methods A **577**, 1 (2007).
[3] H-D. Betz, Rev. Mod. Phys. **44**, 465 (1972).
[4] M. R. Gochitashvili, R. Ya. Kezerashvili, and R. A. Lomsadze, Phys. Rev. A **82**, 022702 (2010).
[5] R. Moshammer *et al.*, Phys. Rev. Lett. **79**, 3621 (1997).
[6] I. D. Kaganovich, E. A. Startsev, and R. C. Davidson, New J. Phys. **8**, 278 (2006).
[7] M. Kireeff Covo, I. D. Kaganovich, A. Shnidman, A. W. Molvik, and J. L. Vujic, Phys. Rev. A **78**, 032709 (2008).
[8] H. Beyer and V. P. Shevelko, *Atomic Physics with Heavy Ions* (Springer, Berlin, 1999).
[9] W. Fischer *et al.*, Phys. Rev. Spec. Top.–Accel. Beams **11**, 041002 (2008).
[10] T. Demma, S. Petracca, F. Ruggiero, G. Rumolo, and F. Zimmermann, Phys. Rev. Spec. Top.–Accel. Beams **10**, 114401 (2007).
[11] I. P. Flaks, B. I. Kikiani, and G. N. Ogurtsov, Tech. Phys. **10**, 1590 (1966) [Zh. Tekh. Fiz. **35**, 2076 (1965)].
[12] V. V. Afrosimov, Yu. S. Gordeev, and V. M. Lavrov, Sov. Phys. JETP Lett. **16**, 341 (1972) [Pisma Zh. Eksp. Teor. Fiz. **16**, 480 (1972)].
[13] V. V. Afrosimov, S. V. Bobashev, Yu.S. Gordeev, and V. M. Lavrov, Sov. Phys. JETP **35**, 34 (1972) [Zh. Exsp. Teor. Fiz. **62**, 61 (1972)].

[14] R. Hegerberg, T. Stefensson, and M. T. Elfort, J. Phys. B **11**, 133 (1978).
[15] G. N. Ogurtsov and B. I. Kikiani, Tech. Phys. **11**, 362 (1966) [Zh. Tekh. Fiz. **36**, 491 (1966)].
[16] D. E. Moe and O. H. Petsch, Phys. Rev. **110**, 1358 (1958).
[17] Yu. F. Bidin and S. S. Godakov, Sov. Phys. JETP Lett. **23**, 518 (1976) [Pisma Zh. Eksp. Teor. Fiz. **23**, 566 (1976)].
[18] V. B. Matveev, S. V. Babashev, and V. M. Dukelski, Sov. Phys. JETP **28**, 404 (1969) [Zh. Eksp. Teor. Fiz. **55**, 781 (1968)].
[19] V. B. Matveev and S. V. Babashev, Sov. Phys. JETP **30**, 829 (1970) [Zh. Eksp. Teor. Fiz. **57**, 1534 (1969)].
[20] J. P. Mouzon, Phys. Rev. **41**, 605 (1932).
[21] Sh. Kita, Sh. Gotoh, T. Tanaka *et al.*, J. Phys. Soc. Jpn. **76**, 044301 (2007).
[22] V. V. Afrosimov, Yu. S. Gordeev, and V. M. Lavrov, Sov. Phys. JETP **41**, 860 (1975) [Zh. Eksp. Teor. Fiz. **68**, 1715 (1975)].
[23] R. A. Lomsadze, M. R. Gochitashvili, R. V. Kvizhinadze, N. O. Mosulishvili, and S. V. Bobashev, Tech. Phys. **52**, 1506 (2007).
[24] Yu. N. Demkov, and I. V. Komarov, Sov. Phys. JETP **23**, 189 (1966) [Zh. Eksp. Teor. Fiz. **50**, 286 (1966)].
[25] E. A. Soloviev, Sov. Phys. JETP **54**, 893 (1981) [Zh. Eksp. Teor. Fiz. **81**, 1681 (1981)].
[26] S. Yu. Ovchinnikov, and E. A. Soloviev, Sov. Phys. JETP **63**, 538 (1986) [Zh. Eksp. Teor. Fiz. **90**, 921 (1986)].
[27] S. Yu. Ovchinnikov, G. N. Ogurtsov, J. H. Macek, and Yu. S. Gordeev, Phys. Rep. **389**, 119 (2004).
[28] P. H. Woerlee, Yu. S. Gordeev, H. Weard, and F. W. Saris, J. Phys. B **14**, 527 (1981).
[29] G. N. Ogurtsov, A. G. Kroupyshev, M. G. Sargsyan, Yu. S. Gordeev, and S. Yu. Ovchinnikov, Phys. Rev. A **53**, 2391 (1996).
[30] G. N. Ogurtsov, A. G. Kroupyshev, and Yu. S. Gordeev, Tech. Phys. Lett. **19**, 711 (1993) [Pisma Zh. Tekh. Fiz. **19**, 20 (1993)].
[31] B. I. Kikiani, R. A. Lomsadze, N. O. Mosulishvili *et al.*, Tech. Phys. **30**, 934 (1985) [Zh. Tekh. Fiz. **55**, 1612 (1985)].
[32] M. R. Gochitashvili, R. A. Lomsadze *et al.*, Georgian Electron. Sci. J.: Phys. (39-2) (2004).
[33] M. R. Gochitashvili, N. Jaliashvili, R. V. Kvizhinadze, and B. I. Kikiani, J. Phys. B **28**, 2453 (1995).
[34] J. M. Ajello and B. Franklin, J. Chem. Phys. **82**, 2519 (1985).
[35] M. J. Mumma and E. C. Zipf, J. Chem. Phys. **55**, 5582 (1971).
[36] E. J. Stone and E. C. Zipf, J. Chem. Phys. **56**, 4646 (1972).
[37] K. H. Tan, F. C. Donaldson, and J. W. McConkey, Can. J. Phys. **52**, 786 (1974).
[38] K. H. Tan and J. W. McConkey, Phys. Rev. A **10**, 1212 (1974).
[39] M. Barat and W. Lichten, Phys. Rev. A **6**, 211 (1972).
[40] E. W. McDaniel, *Collision Phenomena in Ionized Gases* (Wiley, New York, 1964).
[41] V. K. Nikulin, and Yu. N. Tsarev, Chem. Phys. **10**, 433 (1975).
[42] H. Aizawa, K. Wakiya, H. Suzuki *et al.*, J. Phys. B **18**, 289 (1985).
[43] J. Eichler, U. Wille, B. Fastrup, and K. Taulbjerg, Phys. Rev. A **14**, 707 (1976).
[44] D. R. Hartree, *Calculation of Atomic Structures* (Wiley, New York, 1957).
[45] A. A. Radtsig and B. M. Smirnov, *Handbook on Atomic and Molecular Physics* (Atomizdat, Moscow, 1980), Chap. 5, Sec. 5.1.
[46] P. J. Hicks and J. Comer, J. Phys. B **8**, 1866 (1975).
[47] S. Kita, T. Nakamura, A. Watanabe, and N. Shimakura, J. Phys. B **35**, L351 (2002).